AGU PUBLICATIONS

Geophysical Research Letters

RESEARCH LETTER
10.1002/2015GL066888

Key Points:
- Traditional connectivity matrices are limited in displaying temporal variations
- Estuarine connectivity between protected areas varies on multiple time scales
- A novel retention clock concept improves temporal analysis of connectivity

Supporting Information:
- Texts S1 and S2
- Computer Code S1

Correspondence to:
Z. Defne,
zdefne@usgs.gov

Citation:
Defne, Z., N. K. Ganju, and A. Aretxabaleta (2016), Estimating time-dependent connectivity in marine systems, *Geophys. Res. Lett.*, *43*, 1193–1201, doi:10.1002/2015GL066888.

Received 9 NOV 2015
Accepted 12 JAN 2016
Accepted article online 13 JAN 2016
Published online 4 FEB 2016

Estimating time-dependent connectivity in marine systems

Zafer Defne[1,2], Neil K. Ganju[1], and Alfredo Aretxabaleta[1,2]

[1]U.S. Geological Survey, Woods Hole, Massachusetts, USA, [2]Integrated Statistics, Woods Hole, Massachusetts, USA

Abstract Hydrodynamic connectivity describes the sources and destinations of water parcels within a domain over a given time. When combined with biological models, it can be a powerful concept to explain the patterns of constituent dispersal within marine ecosystems. However, providing connectivity metrics for a given domain is a three-dimensional problem: two dimensions in space to define the sources and destinations and a time dimension to evaluate connectivity at varying temporal scales. If the time scale of interest is not predefined, then a general approach is required to describe connectivity over different time scales. For this purpose, we have introduced the concept of a "retention clock" that highlights the change in connectivity through time. Using the example of connectivity between protected areas within Barnegat Bay, New Jersey, we show that a retention clock matrix is an informative tool for multitemporal analysis of connectivity.

1. Introduction

1.1. Connectivity and Time Scales

Hydrodynamic connectivity describes the exchange of water parcels between different regions of a water body. In marine environments this concept has been predominantly applied to studies of larval dispersal using Lagrangian particle tracking to define open versus closed populations, where an open population receives larvae from other sources, while a closed population receives larvae primarily from local spawning [*Mora and Sale*, 2002; *Cowen et al*., 2006, 2007; *Edwards et al*., 2007; *Nanninga et al*., 2015, *Truelove et al*., 2015]. *Cowen et al*. [2007] defined population connectivity as the exchange of individuals between subpopulations separated geographically and proposed its implementation for the design and study of marine protected areas. Biology and complex behaviors (e.g., diel migration and navigation cues) can be added through the use of Lagrangian particle dispersal to produce individual-based models [*Werner et al*., 1993, *Cowen et al*., 2007; *Paris et al*., 2007; *Staaterman et al*., 2012]. The connectivity approach can be extended to other studies that use particle tracking, such as pollutant dispersal [*North et al*., 2011; *Shan and Sheng*, 2012] and sediment transport [*Aretxabaleta et al*., 2014].

The concept of a connectivity matrix was used to display the relation between source and sink locations for fish larvae in the Great Barrier Reef [*James et al*., 2002] and for the exchange of water fractions between different regions of an estuary [*Braunschweig et al*., 2003]. *Mitarai et al*. [2009] provided a probability-based connectivity matrix to distinguish the spatial distribution of particles in the Southern California Bight. While these and other studies [*Watson et al*., 2012; *Narváez et al*., 2012; *Puckett et al*., 2014; *Lough and Aretxabaleta*, 2014; *Kough and Paris*, 2015] have highlighted that time has a large effect on connectivity, a systematic way to represent the temporal component has not been proposed.

Connectivity matrices are a simple way of displaying source-destination relations in a domain for a given time scale when bounded by a specific process (e.g., pelagic larval duration). For a general description of spatiotemporal connectivity, however, connectivity matrices that can incorporate temporal variations are required. For this purpose, we introduce the concept of a "retention clock" that displays the change in particle concentration through time in a specific region. We propose the use of a retention clock matrix (RCM) as an informative tool for a multitemporal analysis of hydrodynamic connectivity. We apply the retention clock concept between protected areas in Barnegat Bay (New Jersey, USA) to demonstrate its utility.

1.2. Study Area

Barnegat Bay is a back-barrier estuary that stretches 70 km along the Atlantic coast of New Jersey (Figure 1). It is a shallow (average depth ~ 1.5 m), microtidal system with restricted exchange with the ocean through

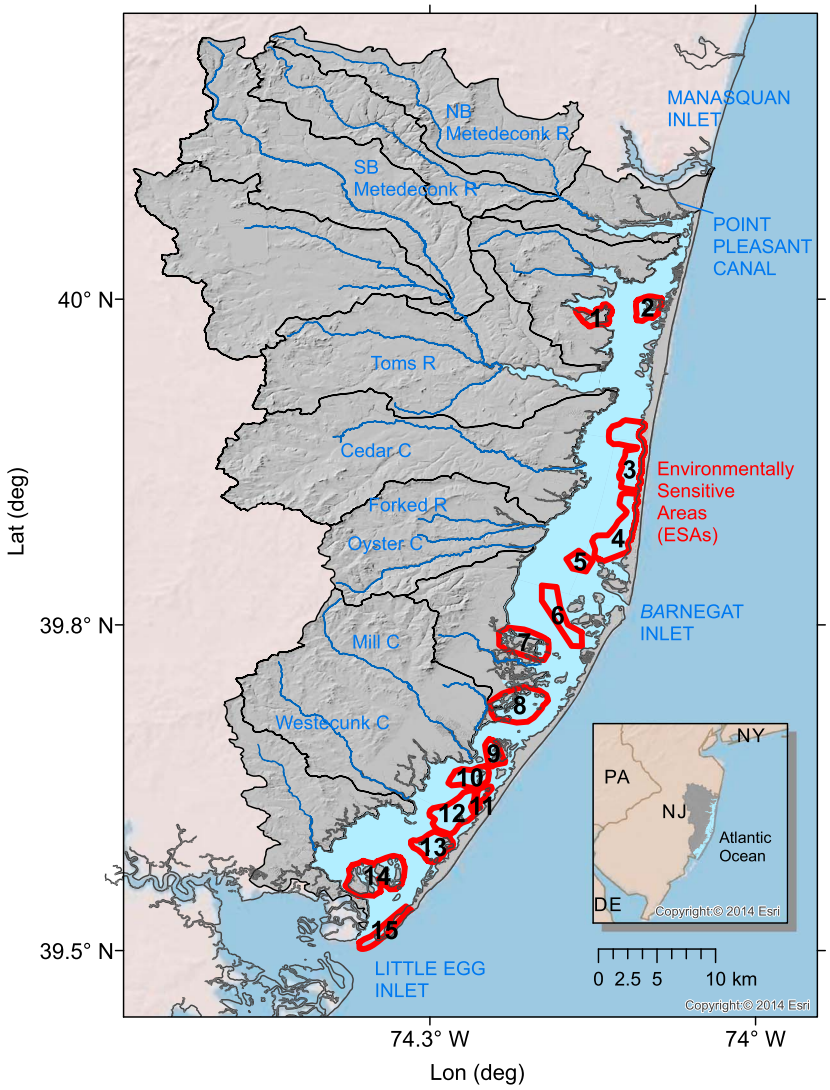

Figure 1. Barnegat Bay (light blue) and its watershed (gray). Environmentally sensitive areas are shown in red.

three openings: Little Egg and Barnegat Inlets and Point Pleasant Canal, which connects Barnegat Bay to Manasquan Inlet. The tidal range attenuates from 1 m to 0.2 m between Little Egg and Barnegat Inlets and to less than 0.2 m north of Barnegat Inlet. The northern half of the bay is less energetic than the southern half and has less exchange with ocean water [*Defne and Ganju*, 2014]. Nutrient loading from the watershed has led to eutrophication, while development has caused loss and alteration of estuarine habitat [*Kennish*, 2001]. To protect submerged habitats, the New Jersey Department of Environmental Protection has defined environmentally sensitive areas (ESAs) within the bay. These are predominantly shallow areas where submerged aquatic vegetation such as eelgrass is found. These areas provide shelter and feeding grounds for numerous fish and wildlife, including shellfish, crabs, and shorebirds [*New Jersey Department of Environmental Protection* (*NJDEP*), 2012].

2. Methodology

2.1. Retention Clock

Considering a single release event of particles in a single, dispersive domain, particle retention can be defined as

$$p = \frac{N(t_i)}{N_0} \tag{1}$$

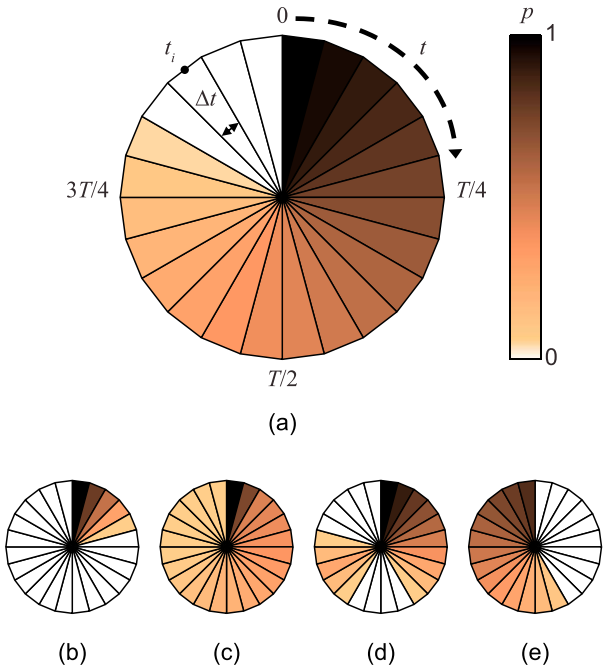

Figure 2. (a) An example retention clock, where time t progresses clockwise from 0 to a time scale T as particle concentration P decreases from 1 to 0. Each slice represents the granularity of temporal resolution Δt centered around time t_i. Retention clock examples for domains with different particle retention characteristics: (b) rapidly dispersing, (c) mostly retaining, (d) both dispersing and recruiting, and (e) recruiting.

where p is a proxy for particle retention based on the concentration of particles in the domain at any given time. $N(t_i)$ represents the number of particles in the domain at time t_i and N_0 is the total number of particles initially released. For the same process, a retention clock can be defined as a circle that spans the entire time scale of interest T, with a given temporal resolution of Δt and p ranging from 1 to 0 (Figure 2a).

Consequently, domains with different retention characteristics have unique retention clocks. For a slowly dispersing domain, the particle concentration, hence the clock, would gradually approach 0 (Figure 2a), whereas for a rapidly dispersing domain the clock would approach 0 faster and a larger portion of the clock would remain at 0 (Figure 2b). The clock for a retentive domain does not reach 0 (Figure 2c). A domain can disperse and recruit particles at different time scales (Figure 2d), or it can be a destination domain where initially, there are no particles and particle concentration increases with the recruitment of new particles (Figure 2e).

By the same token, for each predetermined source, destination, and a maximum time scale, connectivity can be represented in terms of the concentration of particles traveled from a specific source to a specific destination. Therefore, a connectivity proxy can be defined as

$$P(s,d,t_i) = \frac{\overline{N}(s,d,t_i)}{N_0(s)} \tag{2}$$

where $P(s,d,t_i)$ is the connectivity proxy based on concentration of particles from source s at destination d at time t_i, $N_0(s)$ is the total number of particles initially released at s, and $\overline{N}(s,d,t_i)$ is the average number of particles over a period of Δt centered around time t_i:

$$\overline{N}(s,\mathrm{d},t_i) = \frac{1}{\Delta t} \cdot \int_{t_i-\Delta t/2}^{t_i+\Delta t/2} N(s,\mathrm{d},t) \cdot \mathrm{d}t \tag{3}$$

where $N(s,\mathrm{d},t)$ is the instantaneous number of particles from s at d at time t. In this case a source domain can also be a destination with particle concentration decreasing in time, but with a possibility of recruiting new particles (Figure 2d) or solely a destination if no particles were initially released in the domain (Figure 2e). In the case of multiple sources and destinations a retention clock matrix (RCM) can be established to evaluate the connectivity between all pairs. The timing of connectivity between each possible combination of source-destination pairs and its strength can be assessed in a single diagram using the corresponding retention clock. The color intensity shows the strength of connectivity between a pair, with darker colors indicating larger fraction of particles moving from source to destination. Peak time of connectivity can be estimated based on the slice with the darkest color intensity. A retention clock mostly full with varying color intensity means connectivity at multiple time scales, whereas a mostly blank clock indicates weak connectivity between a pair. If there is no significant connectivity (assumed $P = 0.001$ in this study) between a pair, then a retention clock is not displayed. A pseudocode for generating a RCM is provided (Computer Code S1 in the supporting information).

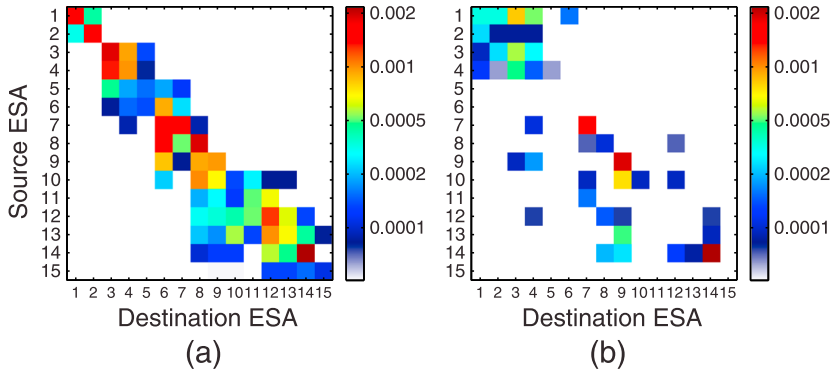

Figure 3. Connectivity matrices for two different time scales for ESAs in Barnegat Bay, NJ, (a) 2 days and (b) 28 days. The color bars indicate particle concentration in logarithmic scale.

2.2. Hydrodynamic Model and Particle Tracking

Circulation in Barnegat Bay was simulated with a 3-D hydrodynamic model for a 70 day period from March to May 2012 [*Defne and Ganju*, 2014] using the Coupled-Ocean-Atmospheric-Wave-Sediment Transport system [*Warner et al*., 2010]. Model forcing at lateral boundaries included river flow data from U.S. Geological Survey stream gages, tidal forcing from ADCIRC regional tide simulation [*Mukai et al*., 2002], salinity, temperature, and tidally averaged water level and barotropic velocity from the Experimental System for Predicting Shelf and Slope Optics model [*Wilkin and Hunter*, 2013]. Atmospheric forcing was applied by bulk formulae from the North American Mesoscale model (http://nomads.ncep.noaa.gov/). The hydrodynamic model had seven evenly distributed vertical layers, a horizontal resolution between 40 and 200 m, and a time step of 5 s. The model skill for hydrodynamics was assessed by *Defne and Ganju* [2014].

We used the LTRANS Lagrangian transport model for particle tracking simulations (*North et al*. [2011], supporting information Text S2). Particles were defined as neutrally buoyant, passive particles with a random displacement for turbulent motion. They were positioned uniformly in the top layer of each ESA polygon with one particle at the central node of each nine neighboring grid nodes (Figure 1). Because the initial time of release with respect to the tidal phase may have a strong influence on the particle path and final destination, the particles were released hourly during a 24 h period (a total of ~14,000 particles). The time is assumed to be 0 at the beginning of each release regardless of the hour of the day, and the particles were tracked until the end of the hydrodynamic simulation.

3. Results and Discussion

The tidal and subtidal dynamics in Barnegat Bay during the simulation period were discussed in *Defne and Ganju* [2014]. To summarize, tidal discharges at Barnegat and Little Egg Inlets were an order of magnitude larger than the tidal discharge at Point Pleasant Canal, and the hydrodynamic model indicated a northward residual circulation from Little Egg Inlet to Barnegat Inlet and Point Pleasant Canal during the simulation period, consistent with prior field studies [*Chant*, 2001]. Because of this residual circulation, northward transport prevailed in Barnegat Bay.

We demonstrate the traditional connectivity matrix approach by applying it at two different time scales: 2 d and 28 d after the initial release (Figure 3). Here the color scale shows the particle concentration at the selected time scale, and because the ESAs were listed as sources on the *y* axis and destinations on the *x* axis, the diagonal shows the retention capacity for each ESA. In the 2 d example, the highest particle concentrations were still predominantly along the diagonal, indicating that the particles were still at the early stages of dispersal at their source ESAs (Figure 3a). Therefore, this time scale can be too short to observe the connectivity between ESAs that are far from each other. Selecting a longer time scale provided a wider spread over the connectivity matrix (Figure 3b). However, at this time scale the spatial coverage is minimal, as only a small fraction of particles remained in the system. Some of the information was already lost; none of the particles from ESAs 5 and 15 remained in the system (Figure 3b). This example highlights that if unbounded by any physical or ecological process, the selection of a time scale is subjective and can limit the analysis or cause

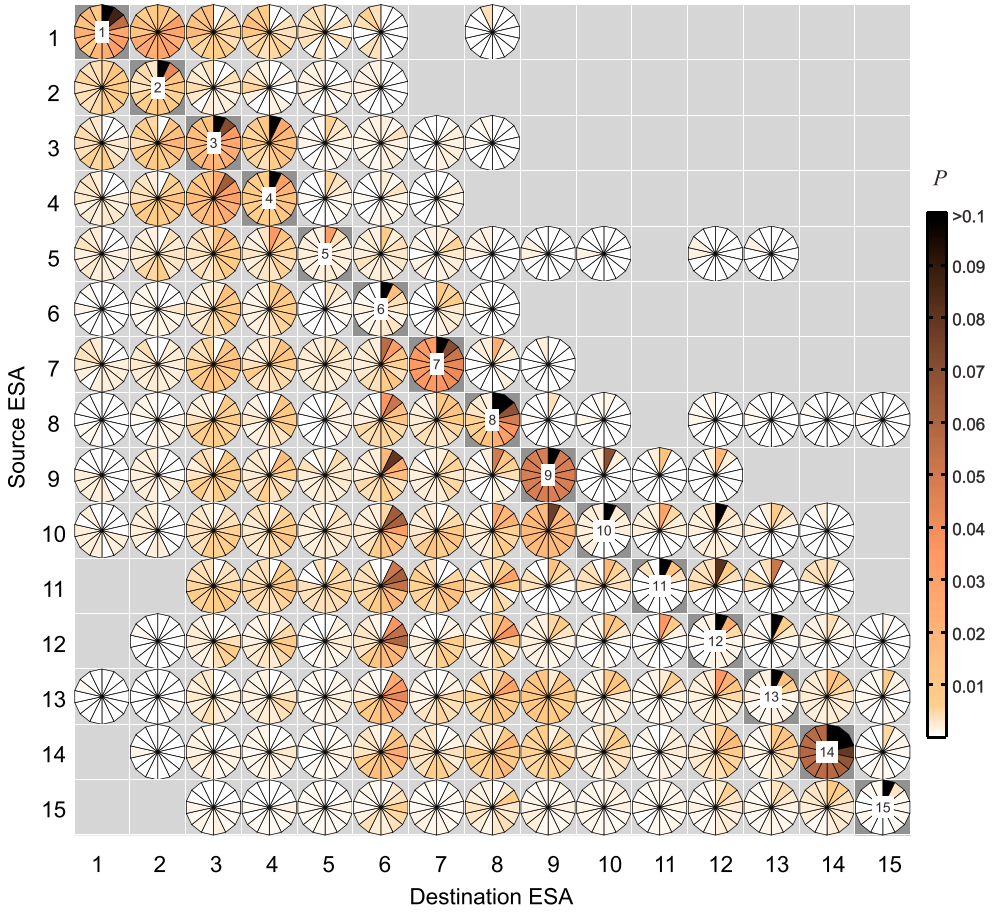

Figure 4. Retention clock matrix (RCM) for ESAs in Barnegat Bay, NJ. The diagonal (dark gray) shows the particle retention capacity for each ESA. Source ESAs are listed according to their increasing labels from north to south.

information loss. It would be more beneficial to preserve temporal information on connectivity while benefiting from the simplicity of a connectivity matrix.

As an alternative to this approach, we have established an RCM for all of the ESAs in Barnegat Bay (Figure 4). The maximum time scale was selected as 28 d, twice the mean residence time for the bay during the study period [*Defne and Ganju*, 2014]. It is possible to interpret the RCM at the estuary scale and recognize general trends or examine each source-destination pair individually to assess the time-dependent connectivity between them. The direction of particle exchange between each pair in Figure 4 is referred in the text with s (*row* #) d (*column*#) indicating particle transport from source (row number) to destination (column number).

Because the source ESAs were numbered from north-to-south, the top right quadrant of the diagram represented transport from the northern half to the southern half of the bay, i.e., particles moving from smaller numbers (s1 through s7) to larger numbers (d9 through d15). At the estuary scale, the effect of the northward residual current appeared as an empty top right quadrant indicating that the particles from some of the northern ESAs were never advected to southern ESAs during the 28 days. The darker color intensity in the matrix also suggested strong connectivity between ESAs 1 and 2 and between ESAs 3 and 4 at all time scales (s1d2, s2d1 and s3d4, s4d3). The retention clocks along the diagonal indicated that ESAs 7, 9, and 14 were the top retaining areas; the particle concentration never reached 0 and was typically greater than at other destinations at any given time scale. Conversely, ESAs 5, 10, and 15 were poor in retaining particles. Particles released in these ESAs dispersed quickly within the first 2 d with minimal return. Characteristics of open (or closed) populations are often influenced by underlying physics [*Nickols et al*., 2015]. Consequently, ESAs 3–6, which were common destinations for particles from all ESAs at various time scales (indicated with full matrix columns in the RCM), should be more favorable for open populations. ESAs 13–15 may harbor

relatively closed populations because they received particles from a limited number of ESAs (fewer retention clocks in columns 13–15). A larger number of clocks in an RCM row imply connectivity and transport to a larger number of ESAs (e.g., ESA14). This suggests that external disturbances in these ESAs are likely to affect more ESAs. In contrast, disturbances in ESAs that are suitable to open population characteristics (e.g., ESA6) can be compensated by advection from a larger number of ESAs.

When the RCM is analyzed for connectivity between a source-destination pair, more specific temporal information becomes available. For example, most of the particles from ESA8 were transported to ESA6 at the end of 4 d (s8d6, second slice), while it required more than 6 d for particles from ESA12 (s12d6, fourth slice). Additionally, *P* within the first 4 d in ESA7 (s8d7, first two slices) was less than *P* in ESA6 at the end of the 4 d (s8d6, second slice). This suggests that only a small portion of the particles from ESA8 traveled through ESA7 on their way to ESA6. Given its geographical location and orientation across the bay, it is reasonable to denote ESA6 as a common destination for the ESAs to the south. However, a small number of particles originating in northern ESAs can also reach ESA6, overcoming the general residual northward transport by following local transport pathways toward the south. Another ESA with a distinctive connectivity pattern was ESA14. It retained most of the particles (s14d14), but once the particles dispersed, they traveled to most of the other ESAs (s14d3 through s14d15). The RCM is effective in capturing these detailed connectivity patterns which may be overlooked in a traditional connectivity matrix.

Restoration of numerous ecological communities in Barnegat Bay (e.g., blue crab and anchovy [*Jivoff and Able*, 2001], winter flounder [*Curran and Able*, 2002], hard clam [*Bricelj et al*., 2001], submerged aquatic vegetation [*Lathrop and Bognar*, 2001; *Bologna et al*., 2007], and shellfish [*Kraeuter et al*., 2003]) depends on improved understanding of marine connectivity in the estuary. Larval durations of these species range from a few days to several months [*Rice*, 1992; *Able and Fahay*, 1998; *Orth and Moore*, 1983]. Our RCM analysis indicated that there was not only noticeably high physical connectivity between some of neighboring ESAs at a range of time scales from days to weeks (e.g., ESAs 1–2 and 3–4) but also relatively higher connectivity between some of the distant areas in comparison to the rest of ESAs (from ESAs 7–14 to ESA6). While neighboring areas provided the largest exchange, exchanges between even more distant ESAs (e.g., s13d6, s14d6, s7d3) were noticed at longer time scales.

For marine protected areas to be successful at conserving marine populations, the selected areas must be self-sustaining or well interconnected [*Planes et al*., 2009; *Harrison et al*., 2012]. Based on hydrodynamic connectivity, the ESAs that are indicated by the RCM as both retaining and recruiting (e.g., ESAs 1–4 and 7–9) are both self-sustaining and well-interconnected areas (lower vulnerability). The preferred destination ESA6 is a well interconnected, but a relatively less self-sustaining area, while ESA14 is a mostly closed population, self-sustaining area (slightly higher vulnerability). ESA15, on the other hand, is neither well connected nor retaining (highest vulnerability). These trends should be tested with models that include the relevant biological model for each individual ecological problem. Passive particle connectivity may be different than connectivity from biophysical models that include specific behavior (e.g., swimming and sinking behaviors) [*Staaterman et al*., 2012; *Zhang et al*., 2015]. Simulations covering longer periods could benefit from the RCM method, because the temporal information can facilitate characterizing time-dependent patterns in connectivity (episodic, seasonal, etc.), reveal important time scales, and improve the design and assessment of protected areas.

As in any other methods to analyze particle modeling results, the robustness of an RCM analysis depends on the parametrization of the underlying particle tracking model (e.g., release depth, magnitude, and integration time [*Simons et al*., 2013]) and the hydrodynamic numerical model (e.g., spatial and temporal resolution [*Putman and He*, 2013]). The other key criteria are choices of maximum time scale, temporal granularity, and delineation of subregions, which depend on the nature of the problem and should be determined on a case-by-case basis. However, in the case of multiple particle releases in time, having a temporal granularity larger than the total duration of the release leads to a robust RCM not affected by the temporal release pattern. When the interval between each release is too large, one can either construct a new RCM for each release if preserving the time stamps and the effect of specific events (e.g., wind, storms, and flood versus ebb tides) is important or create a single RCM after shifting the release times to a common origin (as one would shift the release times for a 24 h, hourly release to exclude the effect of phasing of diurnal tides on connectivity).

To take advantage of the radial time axes in the RCM method, the number of sites needs to be limited to a manageable size. This can be achieved by identifying subregions based on prior geophysical knowledge [*Soto et al*., 2009] or by starting with the maximum number of subregions, calculating a connectivity matrix integrated over the maximum time scale, and removing the subregions with a connectivity below a certain threshold [*James et al*., 2002]. Using connectivity matrices, *Berglund et al*. [2012] showed that a dominant connectivity pattern for a year over more than 5000 sites was limited to only less than 200 of them. For example, assuming that further grouping of these sites into a smaller number of "supersites" is possible, a RCM could be used to analyze biweekly variations in connectivity between these supersites. *Mitarai et al*. [2009] were limited to predetermined time scales (1, 10, and 30 d), and the resulting connectivity patterns were highly variable based on the advection time. Using a RCM could also provide a characterization of the exact timing and duration of high connectivity periods that appeared as single "peaks" in their connectivity matrices. *James et al*. [2002], *Soto et al*. [2009], *Paris et al*. [2007], and *Galindo et al*. [2010] are other examples that might benefit from the explicit representation of the time component of connectivity in the RCM approach.

4. Summary

Traditional connectivity matrices are useful tools to visualize how different subregions of the domain are connected to each other but not practical to assess connectivity at multiple time scales. The temporal dimension is under considered in connectivity studies due to the difficulty of adding an extra dimension. Here we propose a new method to better portray the temporal variability in connectivity and fill this knowledge gap: the retention clock. We have incorporated a time axis to the connectivity matrices with the use of retention clocks, which facilitate assessment of general connectivity trends between multiple subregions at multiple time scales in a single diagram. This method enables analyzing connectivity between source-destination pairs while preserving information on temporal variation when focused on each individual retention clock.

We applied this method with hydrodynamic modeling and Lagrangian particle tracking to study the connectivity among the environmentally sensitive areas (ESAs) in Barnegat Bay, New Jersey. The retention clock matrix (RCM) effectively identified the source-destination relationship between several ESAs at various time scales while capturing the effect of the prevailing northward residual circulation on the connectivity between the ESAs, and distinguishing between ESAs with a potential of supporting open and closed populations. Hydrodynamic connectivity, displaying exchange of water between subregions based on water flow, is an indicator of dispersal from environmental forcing only. To make applied ecological suggestions, biology associated with each ecological problem should be incorporated in the particle tracking simulations. Future applications can benefit from the explicit temporal dimension of RCMs to reveal time-dependent patterns in connectivity (episodic, seasonal, etc.) and determining the prevailing time scales. If paired with field measurements of larval dispersal, the capability of RCM to display variations in time can be useful in improving biological and behavior modules in individual-based models.

Time scale and temporal granularity selection for a RCM depends on the subject of interest and should be determined by the dynamics of the studied process (e.g., the transport rate as well as egg and larval stages if particle behavior is included). The size of the connectivity matrix exhibits quadratic growth, as the number of source and destination domains increases, and it may not be feasible to build a full matrix of retention clocks for a domain with a large number of subregions. However, it is sometimes possible for neighboring subregions of similar connectivity to be grouped in a single larger subregion, or a matrix of retention clocks can be created for a smaller set of selected domains. The proposed method of the retention clock matrix could easily be extended to other fields such as population dynamics, pollutant, and biogenic (e.g., larval) dispersal with critical temporal information by including the appropriate behavior in the particle tracking simulations.

Acknowledgments

Funding was provided by the New Jersey Department of Environmental Protection and the Coastal and Marine Geology Program of the U.S. Geological Survey. We thank Francisco Werner, Ilgar Safak, and Daniel Nowacki for their helpful comments and suggestions. The hydrodynamic and particle tracking model outputs used in this study are available at http://geoport.whoi.edu/thredds/catalog/clay/usgs/users/zdefne/GRL/catalog.html. For questions about the RCM script please contact the corresponding author (zdefne@usgs.gov). The map of Barnegat Bay Environmentally Sensitive Areas is available at USGS Science Base Catalog (https://www.sciencebase.gov/catalog/) with the following disclaimer: "This map was developed using New Jersey Department of Environmental Protection Geographic Information System digital data, but this secondary product has not been verified by NJDEP and is not state-authorized." Any use of trade, firm, or product names is for descriptive purposes only and does not imply endorsement by the U.S. Government.

References

Able, K. W., and M. P. Fahay (1998), *The First Year in the Life of Estuarine Fishes in the Middle Atlantic Bight*, Rutgers Univ. Press, New Brunswick, N. J.

Aretxabaleta, A. L., B. Butman, R. P. Signell, P. S. Dalyander, C. R. Sherwood, V. A. Sheremet, and D. J. McGillicuddy (2014), Near-bottom circulation and dispersion of sediment containing *Alexandrium fundyense* cysts in the Gulf of Maine during 2010–2011, *Deep Sea Res., Part II, 103*, 96–111.

Berglund, M., M. N. Jacobi, and P. Jonsson (2012), Optimal selection of marine protected areas based on connectivity and habitat quality, *Ecol. Modell., 240*, 105–112, doi:10.1016/j.ecolmodel.2012.04.011.

Bologna, P. A., S. Gibbons-Ohr, and M. Downes-Gastrich (2007), Recovery of eelgrass (*Zostera marina*) after a major disturbance event in Little Egg Harbor, New Jersey, USA, *Bull. NJ. Acad. Sci*, *520*, 1–6.
Braunschweig, F., F. Martins, P. Chambel, and R. Neves (2003), A methodology to estimate renewal time scales in estuaries: The Tagus Estuary case, *Ocean Dyn.*, *53*, 137–145.
Bricelj, V., S. MacQuarrie, and R. Schaffner (2001), Differential effects of *Aureococcus anophagefferens* isolates ("brown tide") in unialgal and mixed suspensions on bivalve feeding, *Mar. Biol.*, *139*(4), 605–616.
Chant, R. J. (2001), Tidal and subtidal motion in a shallow bar-built multiple inlet/Bay system, *J. Coastal Res.*, *32*, 102–114.
Cowen, R. K., C. B. Paris, and A. Srinivasan (2006), Scaling of connectivity in marine populations, *Science*, *311*, 522, doi:10.1126/science.1122039.
Cowen, R. K., G. Gawarkiewicz, J. Pineda, S. R. Thorrold, and F. E. Werner (2007), Population connectivity in marine systems: An overview, *Oceanography*, *20*, 14–21.
Curran, M. C., and K. W. Able (2002), Annual stability in the use of coves near inlets as settlement areas for winter flounder (*Pseudopleuronectes americanus*), *Estuaries*, *25*(2), 227–234.
Defne, Z., and N. K. Ganju (2014), Quantifying the residence time and flushing characteristics of a shallow, back-barrier estuary: Application of hydrodynamic and particle tracking models, *Estuaries Coasts*, *38*, 1–16, doi:10.1007/s12237-014-9885-3.
Edwards, K. P., J. Hare, F. E. Werner, and H. E. Seim (2007), Using 2-dimensional dispersal kernels to identify the dominant influences on larval dispersal on continental shelves, *Mar. Ecol. Prog. Ser.*, *352*, 77–87.
Galindo, H. M., A. S. Pfeiffer-Herbert, M. A. McManus, Y. I. Chao, F. E. I. Chai, and S. R. Palumbi (2010), Seascape genetics along a steep cline: Using genetic patterns to test predictions of marine larval dispersal, *Mol. Ecol.*, *19*, 3692–3707, doi:10.1111/j.1365-294X.2010.04694.x.
Harrison, H. B., et al. (2012), Larval export from marine reserves and the recruitment benefit for fish and fisheries, *Curr. Biol.*, *22*(11), 1023–1028, doi:10.1016/j.cub.2012.04.008.
James, M. K., P. R. Armsworth, L. B. Mason, and L. Bode (2002), The structure of reef fish metapopulations: Modelling larval dispersal and retention patterns, *Proc. R. Soc. London B*, *269*, 2079–2086, doi:10.1098/rspb.2002.2128.
Jivoff, P., and K. W. Able (2001), Characterization of the fish and selected decapods in Little Egg Harbor, *J. Coastal Res.*, *32*, 178–196.
Kennish, M. J. (2001), Characterization of the Barnegat Bay–Little Egg Harbor estuary and watershed, *J. Coastal Res.*, *32*, 3–12.
Kough, A. S., and C. B. Paris (2015), The influence of spawning periodicity on population connectivity, *Coral Reefs*, *34*, 753–757.
Kraeuter, J. N., M. J. Kennish, J. Dobarro, S. R. Fegley, and G. E. Flimlin Jr. (2003), Rehabilitation of the northern quahog (hard clam) (*Mercenaria mercenaria*) habitats by shelling—11 years in Barnegat Bay, New Jersey, *J. Shellfish Res.*, *22*(1), 61–67.
Lathrop, R. G., Jr., and J. A. Bognar (2001), Habitat loss and alteration in the Barnegat Bay Region, *J. Coastal Res.*, *32*, 212–228.
Lough, R. G., and A. L. Aretxabaleta (2014), Transport and retention of vertically migrating adult mysid and decapod shrimp in the tidal front on Georges Bank, *Mar. Ecol. Prog. Ser.*, *514*, 119–135.
Mitarai, S., D. A. Siegel, J. R. Watson, C. Dong, and J. C. McWilliams (2009), Quantifying connectivity in the coastal ocean with application to the Southern California Bight, *J. Geophys. Res.*, *114*, C10026, doi:10.1029/2008JC005166.
Mora, C., and P. F. Sale (2002), Are populations of coral reef fish open or closed?, *Trends Ecol Evol.*, *17*, 422–428.
Mukai, A. Y., J. J. Westerink, R. A. Luettich Jr., and D. Mark (2002), Eastcoast 2001: A tidal constituent database for the western North Atlantic, Gulf of Mexico and Caribbean Sea, US Army Engineer Research and Development Center, Coastal and Hydraulics Laboratory, Tech. Rep. ERDC/CHL TR-02-24.
Nanninga, G. B., P. Saenz-Agudelo, P. Zhan, I. Hoteit, and M. L. Berumen (2015), Not finding Nemo: Limited reef-scale retention in a coral reef fish, *Coral Reefs*, *34*, 383–392, doi:10.1007/s00338-015-1266-2.
Narváez, D. A., J. M. Klinck, E. N. Powell, E. E. Hofmann, J. Wilkin, and D. B. Haidvogel (2012), Circulation and behavior controls on dispersal of eastern oyster (*Crassostrea virginica*) larvae in Delaware Bay, *J. Mar. Res.*, *70*(2–3), 411–440.
Nickols, K. J., J. W. White, J. L. Largier, and B. Gaylord (2015), Marine population connectivity: Reconciling large-scale dispersal and high self-retention, *Am. Nat.*, *185*(2), 196–211.
NJDEP (2012), New Jersey Department of Environmental Protection (NJDEP), Green Acres Program, 201210, Barnegat Bay Ecologically Sensitive Areas: NJ Department of Environmental Protection (NJDEP), Trenton, N. J.
North, E. W., E. E. Adams, S. Schlag, C. R. Sherwood, S. Socolofsky, and R. He (2011), Simulating oil droplet dispersal from the Deepwater Horizon spill with a Lagrangian approach, in *Monitoring and Modeling the Deepwater Horizon Oil Spill: A Record Breaking Enterprise*, vol. 195, pp. 217–226, AGU, Washington, D. C.
Orth, R. J., and K. A. Moore (1983), Seed germination and seedling growth of Zostera marina L. (eelgrass) in the Chesapeake Bay, *Aquat. Bot.*, *15*, 117–131.
Paris, C. B., L. M. Chérubin, and R. K. Cowen (2007), Surfing, spinning, or diving from reef to reef: Effects on population connectivity, *Mar. Ecol. Prog. Ser.*, *347*, 285–300, doi:10.3354/meps06985.
Planes, S., G. P. Jones, and S. R. Thorrold (2009), Larval dispersal connects fish populations in a network of marine protected areas, *Proc. Natl. Acad. Sci. U.S.A.*, *106*(14), 5693–5697, doi:10.1073/pnas.0808007106.
Puckett, B. J., D. B. Eggleston, P. C. Kerr, and R. A. Luettich (2014), Larval dispersal and population connectivity among a network of marine reserves, *Fish. Oceanogr.*, *23*(4), 342–361.
Putman, N. F., and R. He (2013), Tracking the long-distance dispersal of marine organisms: sensitivity to ocean model resolution, *J. R. Soc. Interface*, *10*(81), 20120979, doi:10.1098/rsif.2012.0979.
Rice, M. A. (1992), *The Northern Quahog: The Biology of Mercenaria mercenaria*, Rhode Island Sea Grant, Univ. of Rhode Island, Narragansett, Rhode Island.
Shan, S., and J. Sheng (2012), Examination of circulation, flushing time and dispersion in Halifax Harbour of Nova Scotia, *Water Qual. Res. J. Can.*, *47*(3–4), 353–374.
Simons, R. D., D. A. Siegel, and K. S. Brown (2013), Model sensitivity and robustness in the estimation of larval transport: A study of particle tracking parameters, *J. Mar. Syst.*, *119–120*, 19–29, doi:10.1016/j.jmarsys.2013.03.004.
Soto, I., A. Serge, C. Hu, F. E. Muller-Karger, C. C. Wall, J. Sheng, and B. G. Hatcher (2009), Physical connectivity in the Mesoamerican Barrier Reef System inferred from 9 years of ocean color observations, *Coral Reefs*, *28*(2), 415–425, doi:10.1007/s00338-009-0465-0.
Staaterman, E., C. B. Paris, and J. Helgers (2012), Orientation behavior in fish larvae: A missing piece to Hjort's critical period hypothesis, *J. Theor. Biol.*, *304*, 188–196, doi:10.1016/j.jtbi.2012.03.016.
Truelove, N. K., K. Ley-Cooper, I. Segura-García, P. Briones-Fourzán, E. Lozano-Álvarez, B. F. Phillips, S. J. Box, and R. F. Preziosi (2015), Genetic analysis reveals temporal population structure in Caribbean spiny lobster (*Panulirus argus*) within marine protected areas in Mexico, *Fish. Res.*, *172*, 44–49, doi:10.1016/j.fishres.2015.05.029.

Warner, J. C., B. Armstrong, R. He, and J. B. Zambon (2010), Development of a Coupled Ocean–Atmosphere–Wave–Sediment Transport (COAWST) Modeling System, *Ocean Modell.*, *35*(3), 230–244, doi:10.1016/j.ocemod.2010.07.010.

Watson, J. R., B. E. Kendall, D. A. Siegel, and S. Mitarai (2012), Changing seascapes, stochastic connectivity, and marine metapopulation dynamics, *Am. Nat.*, *180*(1), 99–112.

Werner, F. E., F. H. Page, D. R. Lynch, J. W. Loder, R. G. Lough, R. I. Perry, D. A. Greenberg, and M. M. Sinclair (1993), Influences of mean advection and simple behavior on the distribution of cod and haddock early life stages on Georges Bank, *Fish. Oceanogr.*, *2*, 43–64, doi:10.1111/j.1365-2419.1993.tb00120.x.

Wilkin, J. L., and E. J. Hunter (2013), An assessment of the skill of real-time models of Mid-Atlantic Bight continental shelf circulation, *J. Geophys. Res. Oceans*, *118*, 2919–2933, doi:10.1002/jgrc.20223.

Zhang, X., D. Haidvogel, D. Munroe, E. N. Powell, J. Klinck, R. Mann, and F. S. Castruccio (2015), Modeling larval connectivity of the Atlantic surfclams within the Middle Atlantic Bight: Model development, larval dispersal and metapopulation connectivity, *Estuarine Coastal Shelf Sci.*, *153*, 38–53, doi:10.1016/j.ecss.2014.11.033.